Materials Chemistry and Physics 137 (2013) 1073–1080

Contents lists available at SciVerse ScienceDirect

Materials Chemistry and Physics

journal homepage: www.elsevier.com/locate/matchemphys

Nanostructured $Ce_{1-x}Zr_xO_2$ solid solutions produced by mechanochemical processing

I.A. Carbajal-Ramos [a,b,c], J. Andrade-Gamboa [a,c], F.C. Gennari [a,b,c,*]

[a] Instituto Balseiro, Universidad Nacional de Cuyo, Argentina
[b] Consejo Nacional de Investigaciones Científicas y Técnicas (CONICET), Argentina
[c] Centro Atómico Bariloche (Comisión Nacional de Energía Atómica), Argentina

HIGHLIGHTS

- The $Ce_{1-x}Zr_xO_2$ solid solutions ($x \leq 0.2$) are synthesized by mechanochemical processing.
- The synthesis mechanism involves *in-situ* CeO_2 and amorphous ZrO_2 formation.
- The $Ce_{0.8}Zr_{0.2}O_2$ solid solution obtained has high surface area and nanometric grains.
- Addition of an extra amount of NaCl during milling hinders $Ce_{1-x}Zr_xO_2$ formation.
- NaCl removal previous to calcination improves textural/microstructural $Ce_{0.8}Zr_{0.2}O_2$ features.

GRAPHICAL ABSTRACT

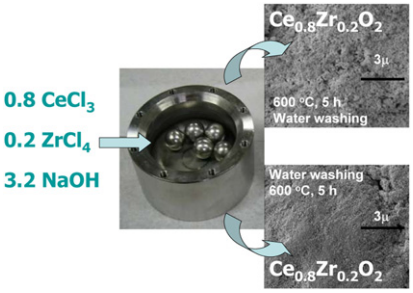

ARTICLE INFO

Article history:
Received 6 June 2012
Received in revised form
9 November 2012
Accepted 11 November 2012

Keywords:
Oxides
Microstructure
Powder diffraction
Nanostructures

ABSTRACT

The nanostructured $Ce_{1-x}Zr_xO_2$ solid solutions ($x \leq 0.2$) have been successfully synthesized from $CeCl_3$–$ZrCl_4$–NaOH mixtures by mechanochemical processing as a gradual transformation, involving *in-situ* CeO_2 and amorphous ZrO_2 formation as intermediates. Solid solutions type-$Ce_{1-x}Zr_xO_2$ along with NaCl as diluent were obtained at different milling times, with a final composition of $Ce_{0.8}Zr_{0.2}O_2$ after 5 h and 15 h under high and low energetic milling conditions, respectively. The NaCl formed during the mechanochemical reaction, which is eliminated by washing after calcination of the as-milled sample, allows to obtain a $Ce_{0.8}Zr_{0.2}O_2$ solid solution with high surface area and nanometric grains. The nanostructured $Ce_{0.8}Zr_{0.2}O_2$ solid solution shows good thermal stability after prolonged heating at 600 °C. However, the addition of an extra amount of diluent during mechanochemical reaction evidences a detrimental effect, avoiding the formation of solid solution or deteriorating the textural/microstructuctural characteristics of the obtained $Ce_{1-x}Zr_xO_2$ solid solution. Removal of NaCl previous to calcination improves notably the textural/microstructural characteristics of the $Ce_{0.8}Zr_{0.2}O_2$ solid solution.

1. Introduction

Ceria-zirconia solid solutions are very attractive materials due to their widespread applications in different fields, such as high-temperature ceramics, catalysis, solid oxide fuel cells (SOFC), gas sensors and polishing materials [1,2]. Two features are mainly

* Corresponding author. Centro Atómico Bariloche (CNEA), R8402AGP, S. C. de Bariloche, Argentina. Tel.: +54 2944 445118; fax: +54 2944 445190.
E-mail address: gennari@cab.cnea.gov.ar (F.C. Gennari).

0254-0584/$ – see front matter © 2012 Elsevier B.V. All rights reserved.
http://dx.doi.org/10.1016/j.matchemphys.2012.11.039

responsible for making ceria-based materials promising for their use as a support and/or as an active catalyst [3,4]. One of these features is the redox couple Ce^{3+}/Ce^{4+}, with the ability of ceria to shift between Ce^{4+} and Ce^{3+} under oxidizing and reducing conditions, respectively. The second one is the easy formation of labile oxygen vacancies and the relatively high mobility of bulk oxygen species. Insertion of ZrO_2 into the CeO_2 modifies ion mobility inside the lattice resulting in the formation of a defective fluorite-structured solid solution. In fact, Zr incorporation into CeO_2 lattice to form $Ce_{1-x}Zr_xO_2$ solid solutions has been proved to significantly improve the catalytic properties, thermal stability and surface area of the resulting material [5,6]. In particular, it has been shown that metal supported on $Ce_{0.8}Zr_{0.2}O_2$ solid solutions are effective redox promoters at low temperatures, being investigated as components/active supports for catalytic processes involved in H_2 production [7], purification by Water Gas Shift (WGS) [8] and CO oxidation [9].

A variety of techniques have been reported for the production of ceria-zirconia solid solutions, such as high temperature solid-state reaction [10], high energy ball milling [11–13], precipitation [14], microwave [15], thermal decomposition of precursors [16], micro-emulsion [17], surfactant-assisted route [18], etc. However, several of these synthesis procedures are energy intensive, produce large amounts of waste, are time-consuming and expensive, mainly when high surface area and small particle size are desired. Moreover, most of these approaches are complicated and possess limitations, such as expensive precursors and limited yield, which made them unsuitable for large scale applications. In this context, mechanochemical processing provides an alternative, room temperature and rapid route to produce nanocrystalline solid materials [19,20]. In this process chemical precursors undergo a reaction, either during milling or during subsequent low temperature heat treatment, to produce the desired material consisting of ultrafine particles embedded within a soluble by-product. Selective removal of the matrix by washing allows recovering an ultrafine powder. Then, this synthesis procedure looks simple and versatile, producing nanosized compounds.

In the last twenty years, mechanochemical processing has been applied to the synthesis of a wide range of ultrafine materials, in particular oxides [19–23]. For instance, both nanocrystalline CeO_2 and ZrO_2 powders have been produced by mechanochemical reaction of different Ce and Zr precursors in the presence of alkaline oxides or hydroxides [24–32]. Although some parameters of the synthesis influence the microstructural and textural features of the final product, the effect of diluent has been mainly studied [24,26,28,29]. During the synthesis of CeO_2, milling with NaCl diluent led to the formation of CeO_2 nanoparticles of ~10 nm, with both higher surface area and smaller crystallite size than those obtained in the absence of diluent [24]. This positive effect was associated to the formation of cerium precursors isolated in the NaCl matrix, which prevents particle sintering during further thermal treatment. In a similar way, in the course of mechanochemical reaction of the $ZrCl_4$–Li_2O–xLiCl mixture it was demonstrated that the average particle size of ZrO_2 decreases with the increase of diluent content [29,30]. Unexpectedly, only two studies on the mechanochemical synthesis of $Ce_{1-x}Zr_xO_2$ solid solution in the zirconia rich zone ($x = 0.85$) has been reported [31,32]. In one case, the precursors $Ce_2(CO_3)_3.8H_2O$ and $ZrOCl_2.3H_2O$ were mixed with excess of ammonia (wet–solid reaction) and submitted to milling, washing and thermal treatment at >500 °C [31]. In the other investigation, hydrated nitrates of $ZrO(NO_3)_2.nH_2O$ and $Ce(NO_3)_3.6H_2O$ were milled in air and further thermally treated between 600 and 1500 °C to produce ZrO_2-based solid solutions [32]. To the author's knowledge there are not any previous investigations on the synthesis by mechanochemical processing of $Ce_{1-x}Zr_xO_2$ solid solutions in the ceria rich regions ($x \leq 0.2$).

In the search for a simple and economical procedure for the synthesis of $Ce_{0.8}Zr_{0.2}O_2$, the mechanochemical reaction of Ce and Zr chlorides in the presence of NaOH emerges as one of the most suitable options: it could proceeds under solvent-free conditions, it is thermodynamically feasible and it is potentially scaleable. In this paper, we report the successful synthesis of nanostructured $Ce_{0.8}Zr_{0.2}O_2$ solid solution by mechanically processing of the $CeCl_3$ and $ZrCl_4$ precursors with NaOH. We examine the effect of the NaCl diluent and the different milling conditions on the structure, microstructure, texture and thermal stability of the $Ce_{0.8}Zr_{0.2}O_2$ solid solution formed. An assessment of the reaction mechanism is also presented.

2. Experimetal procedures

The starting materials used were anhydrous $CeCl_3$ (Aldrich, purity 99.99%), anhydrous $ZrCl_4$ (Merck, purity 99.9%), NaOH (Biopack, purity 98%) and NaCl (Arturo Hirshel, PA). All reactants were weighted in an argon-filled glove box, with moisture maintained below 1 ppm. The milling was carried out in a planetary ball mill (Fritsch Pulverisette P6), using both vial and balls of stainless steel. A ball to powder weight ratio of 80:1 was employed. Mixtures of $CeCl_3$–$ZrCl_4$–NaOH with 0.8:0.2:3.2 mole ratios were mechanically milled in air at room temperature using two different milling conditions: low (L, 200 rpm) and high (H, 400 rpm) energetic modes. These two milling conditions were applied in order to modify the time of the mechanochemical processing and to compare the iron contamination due to the material from the milling media. After milling, the samples were calcined and washed with water in order to eliminate NaCl produced as sub-product of the reaction (LW and HW samples, respectively). Scheme 1 shows the procedures performed and the corresponding samples denominations.

Additional milling runs using different starting mixtures and experimental conditions were performed. First, to understand the pathway of the mechanochemical processing, mixtures of $CeCl_3$–NaOH and $ZrCl_4$–NaOH with 0.8:0.2 mole ratios were individually milled under air atmosphere using high energetic mode (see Scheme 2, CE and ZR samples, respectively). Second, to clarify the role of NaCl as diluent on the microstructural/textural properties of

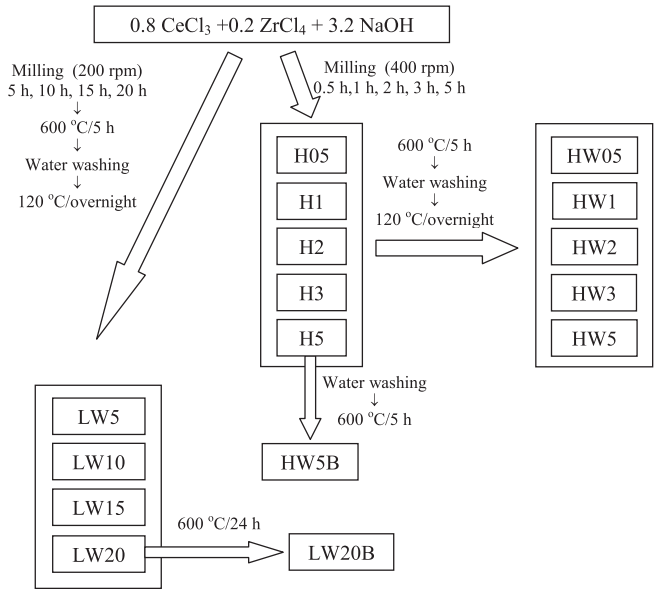

Scheme 1. Procedures for the $Ce_{0.8}Zr_{0.2}O_2$ synthesis using low (L) and high (H) energy milling conditions.

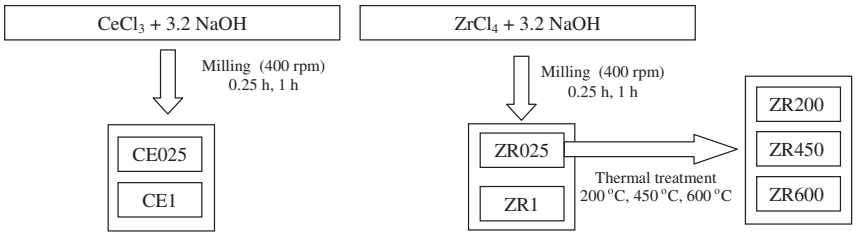

Scheme 2. Procedures corresponding to individual milling of precursors with NaOH.

the final $Ce_{1-x}Zr_xO_2$ solid solution, milling of the $0.8CeCl_3$–$0.2ZrCl_4$–3.2NaOH mixture with an excess of NaCl was performed under low energetic conditions. Scheme 3 summarizes the procedures carried out and the names selected for the samples (LAW samples).

After the milling process the container was opened in order to take the samples for analysis. Structural and microstructural changes were studied by X-ray Powder Diffraction (XRPD, Philips PW 1710/01 Instruments), using CuKα radiation and graphite monochromator. X-ray diffractograms were collected using a step size of 0.025° and a counting time of 1 s. Cell parameters of the solid solution $Ce_xZr_{1-x}O_2$ were calculated with CELREF software [33]. From single peak profile analysis performed on (111) reflection, lorentzian component allowed to calculate mean crystallite size from Scherrer equation and Gaussian component allowed to calculate maximum microstrain as $\varepsilon = \Delta d/d$ [34].

Textural characteristics of the samples were studied using a Micromeritics ASAP 2020 analyzer. N_2 adsorption isotherms were collected at −196 °C on 0.2 g of sample, after evacuation at 350 °C overnight. Surface area and pore distribution were obtained applying the method of Brunauer, Emmett and Teller (BET method) and the method of Barret, Joyner and Halenda (BJH method), respectively. Morphological and chemical analyses of the samples were performed by Scanning Electron Microscopy (SEM Nova Nano 230, FEI Company) equipped with energy dispersive X-ray spectroscopy (EDS) microprobe. The thermal behavior of the samples was studied under argon atmosphere by differential scanning calorimetry (DSC, TA Instruments 2910 calorimeter) using a heating rate of 5 °C min^{-1} and an argon flow rate of 122 ml min^{-1}. About 10 mg of sample was loaded into aluminum capsules. Solid phase infrared spectra were obtained by fourier transform infrared spectroscopy (FTIR) with a Perkin Elmer Spectrum 400 spectrometer in the range of 800–4000 cm^{-1}. The selected samples were grounded with dry KBr, pressed to pellets and put in specially designed cell.

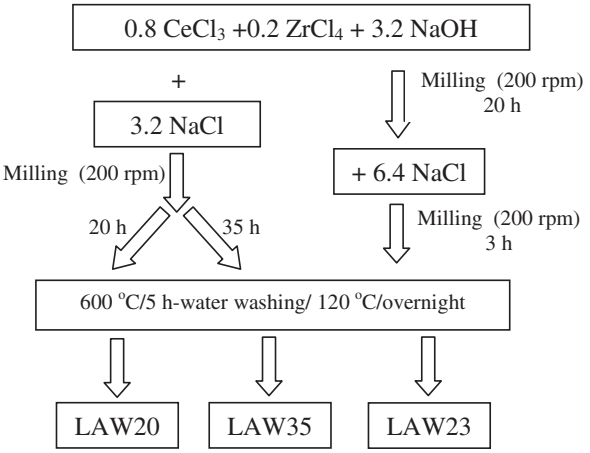

Scheme 3. Procedures to study the effect of NaCl ex situ on the $Ce_{0.8}Zr_{0.2}O_2$ synthesis.

3. Results and discussion

3.1. Mechanochemical processing of the $CeCl_3$–$ZrCl_4$–NaOH mixture (high energetic mode)

Fig. 1 shows the XRPD patterns of the $0.8CeCl_3$–$0.2ZrCl_4$–3.2NaOH mixtures after milling, subsequent heating at 600 °C for 5 h, removal of NaCl by-product phase by washing and drying, as a function of milling time (HW samples). From Fig. 1, two main facts are observed. First, no diffraction peaks corresponding to NaCl are detected, indicating its complete removal during washing. Also, there is no evidence of the presence of tetragonal (t-) or monoclinic (m-) ZrO_2 phases. Second, it can be seen that for the different milling times a cubic fluorite-type structure isomorphic with CeO_2 is obtained. By comparison with the standard CeO_2 (PDF 34–0394) and $Ce_{0.75}Zr_{0.25}O_2$ (PDF 28–0271), we deduce that as the milling time progresses, the starting CeO_2 fluorite-type structure progressively moves to greater 2θ values. This result means Zr incorporation according to Vegard's rule, where linear decrease of the lattice parameter with x in $Ce_{1-x}Zr_xO_2$ is expected because the Zr^{4+} radius (0.84 Å) is less than that of Ce^{4+} (0.97 Å). The x value was calculated by using the relationship $a_x = a_0 - 0.27\,x$ [35], where a_0 and a_x are the cell parameters (in Å) for pure CeO_2 and solid solutions, respectively.

Table 1 summarizes the structural, microstructural and textural data for HW samples after different milling times. From Table 1, it is observed that mean crystallite sizes are in the nanometer range

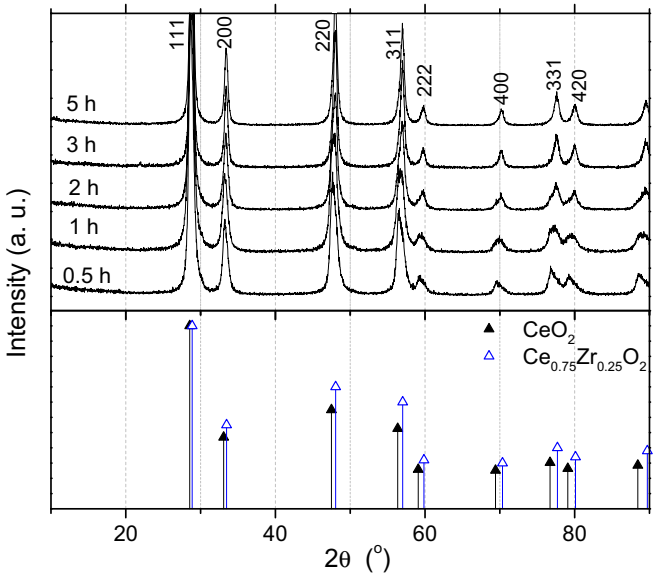

Fig. 1. XRPD patterns of $0.8CeCl_3$–$0.2ZrCl_4$–3.2NaOH mixtures (HW samples) after milling in air for different times, followed by heating at 600 °C for 5 h, washing and subsequent drying.

(15–27 nm), microstrain decreases as milling times increase and x value converges to the expected value for bulk $Ce_{0.8}Zr_{0.2}O_2$ composition (a = 5.357 Å) after 5 h of milling. All these results are consistent with the formation of nanostructured fluorite type-cubic solid solution as consequence of the mechanochemical processing of the $CeCl_3$–$ZrCl_4$–NaOH mixture, followed by thermal treatment at 600 °C for 5 h and subsequent washing.

Fig. 2 shows the SEM micrographs of $Ce_{0.8}Zr_{0.2}O_2$ powders prepared by energetic milling, heating and subsequent washing. Fig. 2A displays the general morphology of the powders, consisting of several rounded agglomerates with sizes between 5 and 50 μm. A detailed inspection of the surface of an agglomerate shows that it contains several small particles of ≈0.2 μm (Fig. 2B). It is worth remarking that the average particle size is much larger than the mean crystallite size (about 17 nm), indicating that ceria-zirconia particles are polycrystalline. Textural characterizations of the HW samples as a function of milling time are also presented in Table 1 (isotherms not shown). The as-synthesized $Ce_{1-x}Zr_xO_2$ solid solutions show Type II isotherms, which indicate the presence of macropores and some mesopores with not well defined size and shape [36]. All fresh samples have high surface area, with values oscillating between 22 and 30 $m^2\ g^{-1}$. As a general tendency, the introduction of the Zr^{4+} into CeO_2 decreases the surface area, with average pore size > 50 nm.

Therefore, the reaction that occurs during the mechanochemical processing of the $0.8CeCl_3$–$0.2ZrCl_4$–3.2NaOH mixture for 5 h can be expressed as:

$$0.8\ CeCl_3(s) + 0.2\ ZrCl_4(s) + 3.2\ NaOH(s) + 0.2O_2(g) \rightarrow Ce_{0.8}Zr_{0.2}O_2 + 1.6H_2O\ (l) + 3.2\ NaCl(s) \quad (1)$$

The reaction (1) is expected to be strongly exothermic at room temperature taking into account the highly negative reaction enthalpy ($\Delta H = -464\ kJ\ mol^{-1}$) [37] to produce $0.8CeO_2 + 0.2ZrO_2$ instead $Ce_{0.8}Zr_{0.2}O_2$. However, the reaction seems to extend to a small volume during each collision resulting in a gradual transformation. In fact, in the present work we find no experimental evidence of self-propagating exothermic reaction. Then, this synthesis procedure allows to gradually produce $Ce_{0.8}Zr_{0.2}O_2$ solid solution, with a high surface area of 26 $m^2.gr^{-1}$, macroporosity (pore size > 50 nm) and mean grain size of 17 nm.

3.2. Formation mechanism of $Ce_{0.8}Zr_{0.2}O_2$ solid solution: identification of intermediate species

To understand the mechanism of the mechanochemical reaction, we perform the milling of $CeCl_3$–NaOH mixture (CE samples) and $ZrCl_4$–NaOH (ZR samples) under high energetic conditions (see Scheme 2). Fig. 3 shows the XRPD patterns of the CE samples after milling for 0.25 and 1 h. It can be seen clearly the formation of NaCl from only 0.25 h of milling, indicating that the reaction between

Table 1
Structural, microstructural and textural parameters of the HW samples (high energetic mode of milling).

Sample	Milling time (h)	Crystallite size (nm)	Microstrain, ε	Cell parameter (Å)	x	Specific surface area (BET, ($m^2\ g^{-1}$)
HW05	0.5	25	0.009	5.402	0.03	30
HW1	1	27	0.010	5.390	0.08	22
HW2	2	19	0.007	5.362	0.18	24
HW3	3	15	0.004	5.366	0.17	29
HW5	5	17	0.003	5.357	0.20	26

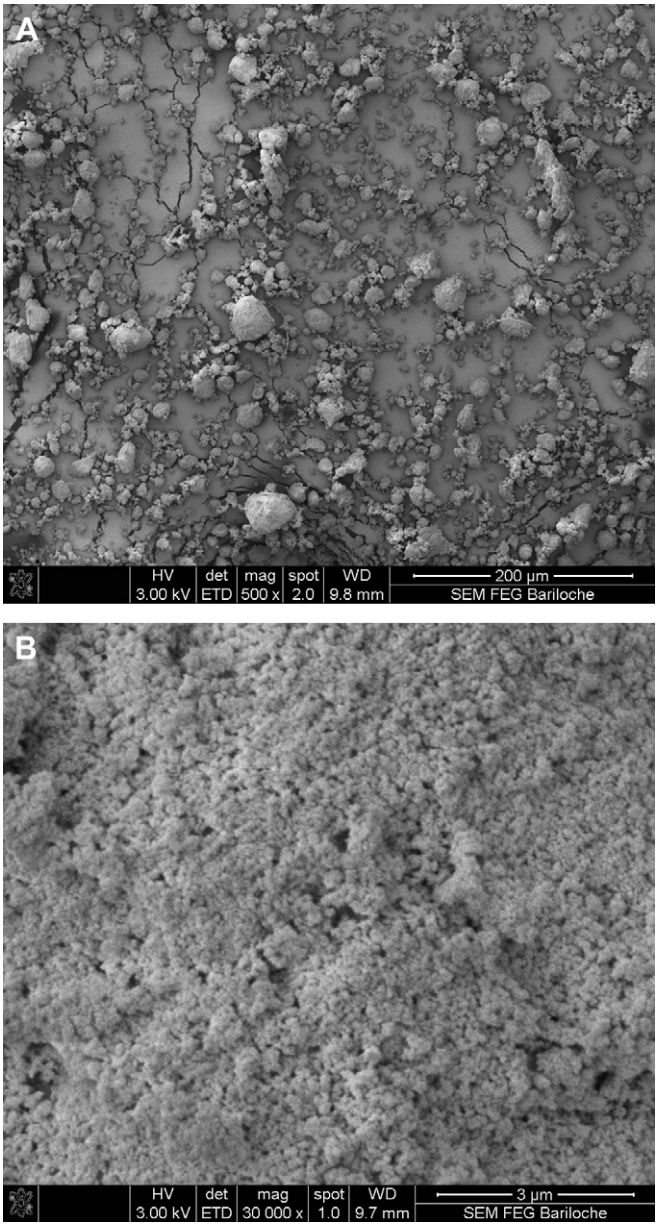

Fig. 2. SEM micrographs of the $Ce_{0.8}Zr_{0.2}O_2$ solid solution produced by mechanochemical processing (HW5 sample). (A) Agglomerate size distribution. (B) Detail of the surface of an agglomerate.

$CeCl_3$ and NaOH has happened. Simultaneously, we observe the formation of $Ce(OH)_3$ (PDF 19–0284) and CeO_2 (PDF 34–0394), while the most intense peaks corresponding to the $CeCl_3$ starting material are not detected. Assuming that for any milling time $CeCl_3$ is completely consumed, the decrease of relative intensity of reflection of $Ce(OH)_3$ at $2\theta \sim 15.8^\circ$ with the increase of milling time suggests the following reactions:

$$CeCl_3(s) + 3NaOH(s) \rightarrow Ce(OH)_3(s) + 3NaCl(s) \quad (2)$$

$$Ce(OH)_3(s) + 0.25O_2(g) \rightarrow CeO_2\ (s) + 1.5H_2O\ (l) \quad (3)$$

which are in agreement with reported results of milling $CeCl_3$–NaOH mixture in Ar, an subsequent calcination in air [24]. In that work, reaction (2) occurred during milling and further heating in air produces CeO_2 according to reaction (3). In the present work,

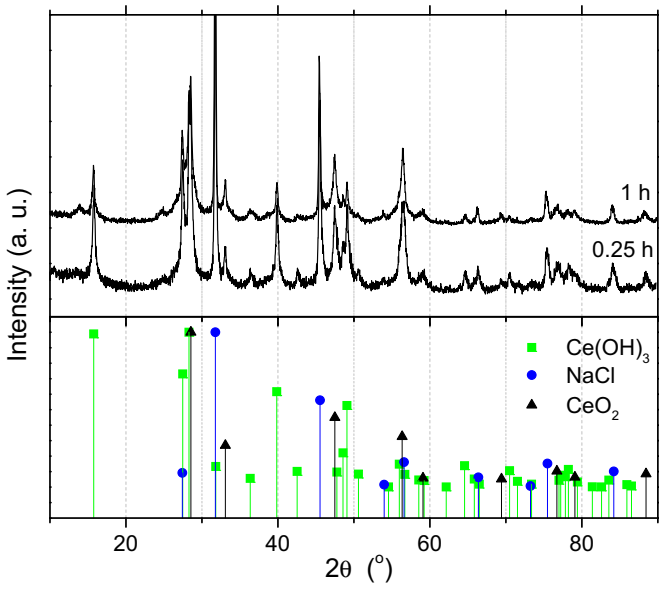

Fig. 3. XRPD patterns of the $CeCl_3$–3.2NaOH mixtures (CE samples) after milling for 0.25 h and 1 h in air.

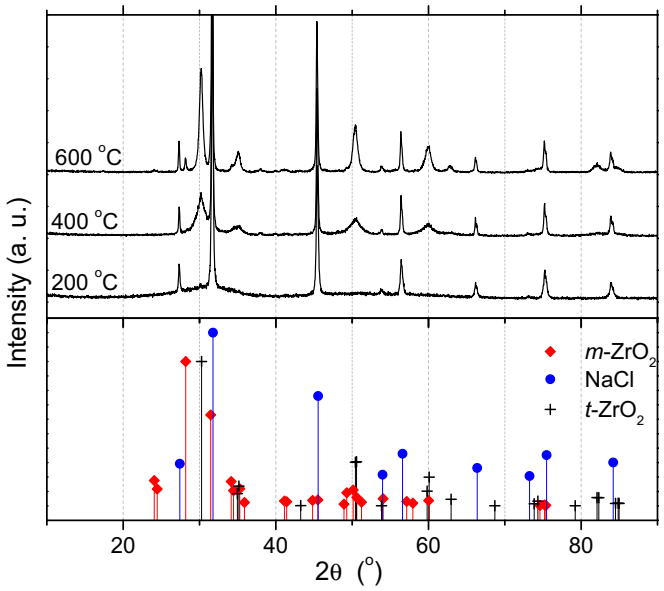

Fig. 5. XRPD patterns of the $ZrCl_4$–3.2NaOH mixture (ZR samples) after milling and heated up to 200, 400 and 600 °C.

since milling was performed in air atmosphere, both processes (reactions (2) and (3)) occur simultaneously previous to the heating.

In the case of the ZR samples, the mechanochemical processing for 0.25 and 1 h conduces to the formation of crystalline NaCl and an amorphous component containing Zr (XRPD patterns not shown). The observation of NaCl diffraction peaks clearly evidences that a reaction between $ZrCl_4$ and NaOH has occurred. To clarify the nature of this interaction, thermal analysis of ZR samples was performed using DSC (Fig. 4). For both ZR samples two thermal events centered at 100 °C and 360 °C are observed. Hence, the ZR sample milled for 0.25 h was submitted to thermal treatments up to the end of each thermal event, *i.e.* 200 °C, 450 °C and 600 °C (indicated by arrows in Fig. 4). Fig. 5 shows the XRPD after thermal treatments at different temperatures (ZR200, ZR450, ZR600 samples). The heating of ZR05 sample up to 200 °C produces only minor structural changes in the sample, and the only crystalline phase detected is NaCl. However, the heating up to 450 °C induces the formation of t-ZrO_2, whereas the thermal treatment at 600 °C leads to the formation of both t-ZrO_2 and m-ZrO_2 phases. Therefore, at 200 °C the main thermal processing involved is the dehydration. As an interesting result, at 450 °C the amorphous component containing Zr transforms to t-ZrO_2. This behavior resembles that of amorphous ZrO_2 on heating [38]. Then, the amorphous component containing Zr must be amorphous ZrO_2. Additional heating at 600 °C induces the transformation from t-ZrO_2 to m-ZrO_2, which is the thermodynamically stable phase.

Supplementary studies were carried out to reinforce the above interpretations. The IR spectra of as-milled ZR samples for 0.25 and 1 h are shown in Fig. 6. The broad band at 3350 cm^{-1} corresponds to the stretching vibrations ν_{OH} of the hydroxyl groups, mainly onto amorphous ZrO_2. The band at 1660 cm^{-1} is due to the bending vibrations of ν_{OHO} of adsorbed water. Although the presence of carbonates cannot be excluded (1550–1450 cm^{-1}), the band at 1405 cm^{-1} is characteristic of the t-ZrO_2 [39]. From comparison of the spectra, we can observe that the ν_{OH} band has higher intensity for the sample milled for a shorter time. Considering that the intensity of this band decreases with the milling, the fraction of amorphous ZrO_2 is reduced from ZR025 to ZR1 [40]. Then, the interaction between $ZrCl_4$ and NaOH can be expressed:

$$ZrCl_4(s) + 4NaOH(s) \rightarrow ZrO_2(s) + 3NaCl(s) + 2H_2O(l) \quad (4)$$

where $ZrO_2(s)$ denotes a zirconia phase which is mainly the amorphous one.

On the basis of the above results (Figs. 3–6), the proposed mechanism for the synthesis of $Ce_{0.8}Zr_{0.2}O_2$ solid solution by mechanochemical processing is the following:

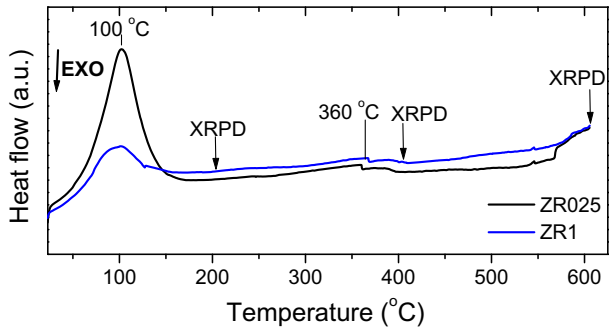

Fig. 4. DSC curves of the $ZrCl_4$–3.2NaOH mixtures (ZR samples) after milling for 0.25 h and 1 h in air. Heating ramp of 5 °C min^{-1} under argon flow.

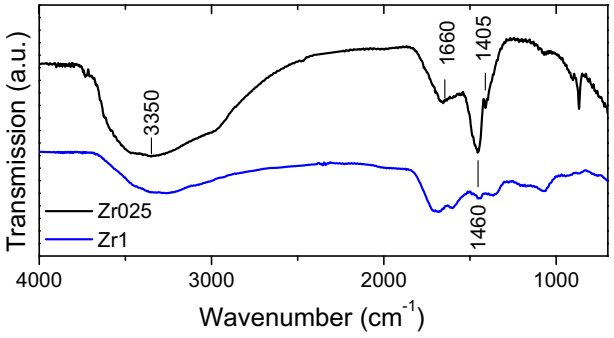

Fig. 6. FTIR spectra of the $ZrCl_4$–3.2NaOH mixtures (ZR samples) after milling for 0.25 h and 1 h in air.

$$0.8CeCl_3(s) + 2.4NaOH(s) + 0.2O_2(g) \rightarrow 0.8CeO_2 + 1.2H_2O\ (l) + 2.4NaCl(s)\ \Delta G^\circ = -418\ kJ\ mol^{-1}\ CeO_2\ [37] \quad (5)$$

$$0.2ZrCl_4(s) + 0.8NaOH(s) \rightarrow 0.2ZrO_2(s) + 0.4H_2O\ (l) + 0.8NaCl(s)\ \Delta G^\circ = -645\ kJ\ mol^{-1}\ ZrO_2\ [37] \quad (6)$$

$$0.8CeO_2(s) + 0.2ZrO_2(s) \rightarrow Ce_{0.8}Zr_{0.2}O_2(s) \quad (7)$$

Taking into account that the $Ce_{0.8}Zr_{0.2}O_2$ solid solution is stable at room temperature [41], it is expected a negative ΔG° for the global reaction, *i.e.* the sum of reactions (5) and (6) that is equal to reaction (1). Then, the overall reaction has much greater driving force than reaction (7) towards the formation of $Ce_{0.8}Zr_{0.2}O_2$. In addition, a kinetic enhancement can be expected due to the amorphous ZrO_2 formed by reaction (4), which must be the most reactive ZrO_2 phase. The high observed reaction rate, compared with other solid–solid synthesis, could be explained assuming amorphous ZrO_2 as the main Zr precursor.

3.3. Mechanochemical processing of the $CeCl_3$–$ZrCl_4$–NaOH mixture (low energetic mode): effect of milling conditions

In order to compare the effect of different energetic modes on the synthesis of the $Ce_{0.8}Zr_{0.2}O_2$ solid solution, the XRPD patterns obtained for the $0.8CeCl_3$–$0.2ZrCl_4$–3.2NaOH mixture after low energetic milling and subsequent heating at 600 °C for 5 h, removal of NaCl by-product phase by washing and drying, are presented in Fig. 7 (LW samples). Similarly to Fig. 1, the progressive incorporation of Zr^{+4} in the cubic structure of CeO_2 leads to a shift in the 2θ position to higher values. Table 2 summarizes structural, microstructural and textural data for LW samples after different milling times. From Table 2, and likewise HW samples, it is observed that mean crystallite sizes are in the nanometer range (~10 nm), microstrain decreases as milling times increase and after 15 h of milling, the formation of $Ce_{0.8}Zr_{0.2}O_2$ is confirmed. Additional milling up to 20 h does not introduce significant structural changes in the solid solution (see Table 2). The nitrogen adsorption isotherm for the $Ce_{0.8}Zr_{0.2}O_2$ sample after 20 h of milling is similar to that

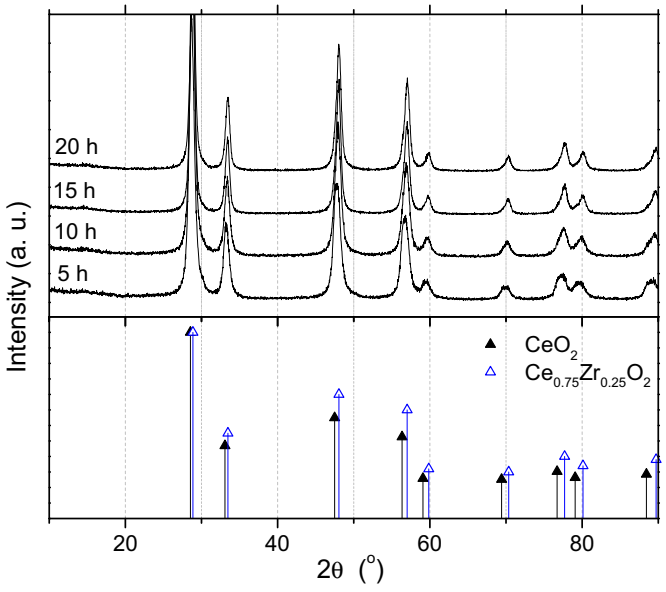

Fig. 7. XRPD patterns of $0.8CeCl_3$–$0.2ZrCl_4$–3.2NaOH mixtures (LW samples) after milling in air for different times, followed by heating at 600 °C for 5 h, washing and subsequent drying.

Table 2
Structural, microstructural and textural parameters of the LW samples (low energetic mode of milling).

Sample	Milling time (h)	Crystallite size (nm)	Microstrain, ε (%)	Cell parameter (Å)	x	Specific surface area (BET, ($m^2\ g^{-1}$)
LW5	5	9	0.006	5.382	0.11	–
LW10	10	9	0.004	5.368	0.16	–
LW15	15	11	0.003	5.357	0.20	24
LW20	20	11	0.002	5.357	0.20	28

obtained by using high energetic milling, obtaining a specific surface area of 28 $cm^2\ g^{-1}$. To analyze the thermal stability of the $Ce_{0.8}Zr_{0.2}O_2$ solid solution produced under low energetic milling, we submitted the sample LW20 to an additional thermal treatment at 600 °C for 24 h. The structural, microstructural and textural features were identical to those of LW20 sample. Then, the synthesized $Ce_{0.8}Zr_{0.2}O_2$ solid solution shows good stability at 600 °C. This temperature is in the order of those used for catalytic applications, such as ethanol steam reforming for hydrogen production [7].

In order to evaluate the contamination of the $Ce_{0.8}Zr_{0.2}O_2$ solid solution produced under low and high energetic milling, chemical composition of the samples was analyzed by EDS on SEM. From EDS analysis performed on various areas of 100 × 100 μm, average values of 78 at.% of Ce, 17 at.% of Zr and 5 at.% of Fe were obtained for HW5 sample. In the case of LW20 sample, the elemental average composition determined was 78 at.% of Ce, 20 at.% of Zr and 2 at.% of Fe. In both cases, the measured elemental percentages are in agreement with nominal composition of the starting mixture (80 at. % Ce–20 at. % Zr). The detection of minor amounts of Fe is not an indication *per se* of its incorporation in the lattice of the solid solution. Considering that the cell parameter of the solid solution indicates a degree of Zr/Ce substitution that agrees with the nominal composition, this incorporation was neglected. However, this fact cannot be ruled out.

Then, the $Ce_{0.8}Zr_{0.2}O_2$ solid solutions obtained by mechanochemical processing display similar specific surface area and pore volume, independently of energetic milling mode applied. As interesting result, the high energetic mode allows to produce the $Ce_{0.8}Zr_{0.2}O_2$ solid solution in shorter milling time. In addition, the iron contamination introduced during high energetic mode is about the same order than that obtained under low energetic mode. As an alternative, minimization of the Fe contamination during mechanochemical activation can be obtained by using wear-resistant milling vial and balls.

3.4. Effect of the diluent

To investigate the effect of diluent on the microstructural, structural and textural characteristics of the material synthesized by mechanochemical process, the same moles of NaCl produced by reaction (1) were initially added. The starting mixture $0.8CeCl_3$–$0.2ZrCl_4$–3.2NaOH was milled with 3.2 NaCl using low energetic mode for 20 and 35 h. Although 15 h of mechanochemical milling using low energetic mode were enough to synthesize the $Ce_{0.8}Zr_{0.2}O_2$ (Fig. 2), for samples with NaCl added, half amount of Zr^{4+} is incorporated into CeO_2 after 20 h of milling (see Table 3). Moreover, additional milling up to 35 h does not produce the $Ce_{0.8}Zr_{0.2}O_2$. Then, the evidence suggests that NaCl acts as an inert phase that prevents the contact between the reactants and/or influence the energy transferred to the reactants

Table 3
Some parameters of the LAW samples (low energetic mode of milling).

Sample	Milling time (h)	Cell parameter (Å)	x	Specific surface area (BET, ($m^2\ g^{-1}$))
LAW20	20	5.384	0.10	24
LAW35	35	5.368	0.16	23
LAW23	23	5.360	0.19	27

during the mechanochemical activation. On the other hand, the BET surface area obtained from the N_2 isotherms were of the same order (between 23 and 28 $m^2\ g^{-1}$) for the samples milled without and with NaCl (Table 3). This evidences that the *ex situ* addition of NaCl does not induce an increment of the BET surface area of the final $Ce_{1-x}Zr_xO_2$ solid solution.

Another milling run was performed to analyze if the presence of an extra amount of NaCl during the calcination could favor high surface area after washing. A sample obtained after the same milling procedure as for LW20 was prepared (see Section 3.2), but previously to calcination/washing steps, 6.4 mol of NaCl were added and additional milling for 3 h was performed. As shown in Table 3, final material (LAW23) possesses practically the same structural and textural characteristics than the LW20 sample (Table 2), *i.e.* without NaCl addition. Therefore, any of the runs proposed in this work evidence a positive role of the NaCl on structural/textural characteristics of the $Ce_{0.8}Zr_{0.2}O_2$ solid solution.

Additionally, we analyze the effect to perform the washing step immediately after milling, *i.e.* avoiding the presence of NaCl during thermal treatment, on the characteristics of the $Ce_{1-x}Zr_xO_2$ solid solution formed. For a sample obtained under the same milling conditions of HW5 sample, calcination-washing sequence was reversed (sample HW5B, see Scheme 1). This procedure leads to the successful formation of $Ce_{0.8}Zr_{0.2}O_2$ solid solution with suitable textural properties and microstructural characteristics. Fig. 8 shows the N_2 adsorption/desorption isotherm for the HW5B sample. To compare, the N_2 isotherm for the HW5 sample is also included. The HW5B sample is highly porous with Type IV isotherms, indicating the presence of a mesoporous network. The specific surface area obtained (BET surface area of 50 $m^2\ gr^{-1}$) was about two times higher than HW5, obtained by calcinations in the presence of NaCl. In addition, by applying the BJH method to the desorption branch of the isotherm (see inset plot Fig. 8), HW5 shows narrow pore size distribution (from 10 to 20 nm), whereas the HW5 sample possesses macropores >50 nm. Then, a notable improvement in the microstructural and textural characteristics of the $Ce_{0.8}Zr_{0.2}O_2$ solid solution is reached by a simple modification

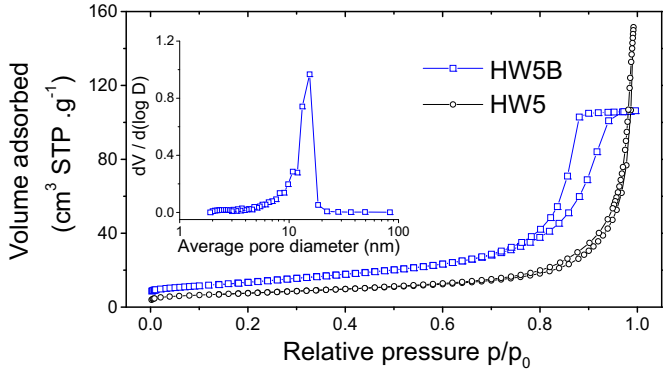

Fig. 8. Nitrogen adsorption/desorption isotherms for HW5 and HW5B samples. Inset plot shows pore-size distribution of the HW5B sample.

in the synthesis procedure: to perform calcinations after removing NaCl formed during milling process. Fig. 9 shows the morphology of the $Ce_{0.8}Zr_{0.2}O_2$ powders obtained applying this procedure. By comparison with Fig. 2, the morphology of the powders notably changes towards big agglomerates of >200 μm (Fig. 9A), with non-uniform shape. However, an inspection of the surface revels that it is constituted by micrometric rounded particles of <0.2 μm, uniform in size and shape (Fig. 9B). Then, the NaCl elimination before thermal treatment clearly favors the agglomeration but generates a spongy surface, with the consequent higher surface area.

An analysis of the techniques reported for the production of $Ce_{2-x}Zr_xO_2$ solid solutions, reveals that the high temperature solid-state procedure leads to a final material with poorer microstructural features [10], while wet chemistry routes allow the production of $Ce_{2-x}Zr_xO_2$ nanostructured, with high

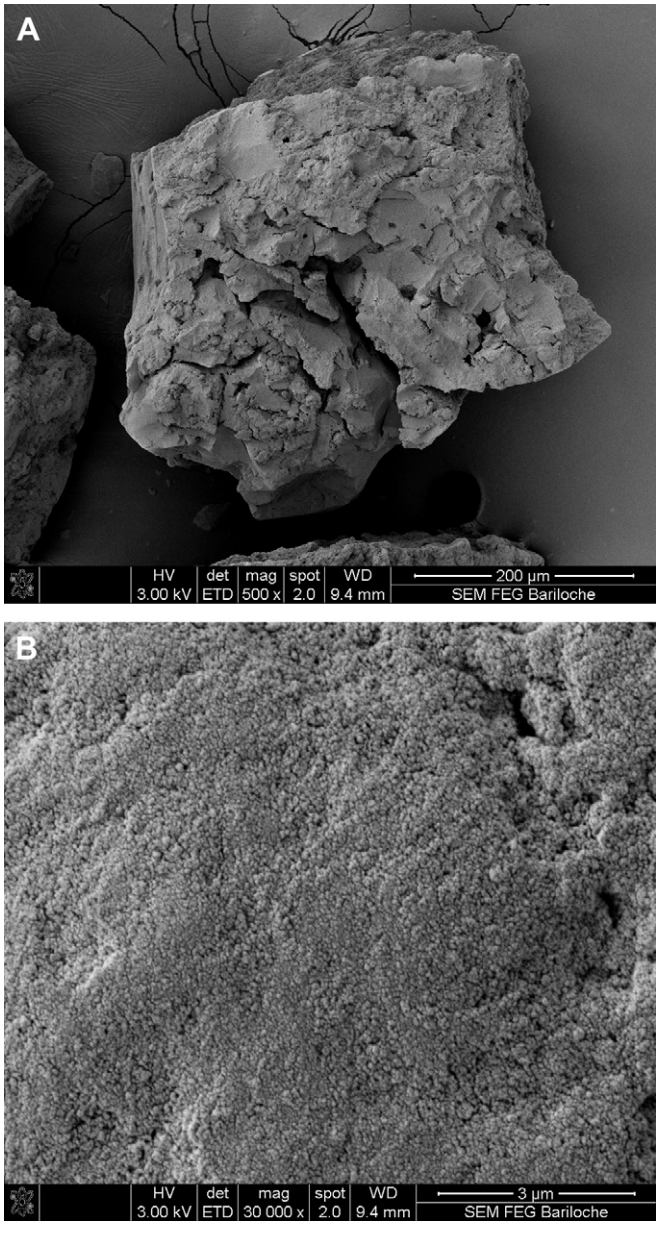

Fig. 9. SEM micrographs of the $Ce_{0.8}Zr_{0.2}O_2$ solid solution produced by mechano-chemical processing (HW5B sample). (A) Agglomerate morphology. (B) Detail of the surface of the agglomerate.

surface areas [14–18]. Regarding the application of other solid-state routes, Chen et al. [11] were the first to report the formation of $Ce_{2-x}Zr_xO_2$ by mechanical milling of the CeO_2–ZrO_2 mixture. They obtained the $Ce_{0.7}Zr_{0.3}O_2$ solid solution after 60 h of milling, with a lattice parameter of $a = 0.530$ nm. No additional characterization of the final material was performed. In a subsequent work, the milling of CeO_2 powders using balls and container of ZrO_2 allowed the formation of $Ce_{2-x}Zr_xO_2$ [13]. However, as the milling time progresses, Zr content in the solid solution increases and specific surface area decreases. Finally, Trovarelli et al. [12] synthesized the $Ce_{0.8}Zr_{0.2}O_2$ solid solution through high energy milling of the CeO_2–ZrO_2 mixture by 12 h. The final material without calcination had a lattice parameter of $a = 0.5336(8)$ nm, with a surface area of 27–33 $m^2\ g^{-1}$ and grain sizes ranging from 4 to15 nm. In the present work, we were able to produce a $Ce_{0.8}Zr_{0.2}O_2$ solid solution by mechanochemical processing for 5 h and additional heating at 600 °C, with lattice parameter and nanometric grains similar to those reported by Trovarelli [12], but with an improved surface area (50 $m^2\ g^{-1}$). Taking into account the final textural/microstructural characteristics reached for $Ce_{0.8}Zr_{0.2}O_2$, the mechanochemical route presented in this work constitutes a simple, rapid and economic method for the fruitful production of $Ce_{2-x}Zr_xO_2$ solid solutions.

4. Summary and conclusions

Fluorite type $Ce_{0.8}Zr_{0.2}O_2$ solid solution was successfully synthesized by mechanochemical processing of the $0.8CeCl_3$–$0.2ZrCl_4$–3.2NaOH mixture at room temperature, for both high and low energetic modes. The global mechanochemical reaction can be interpreted as the sum of two different reactions. First, the milling induces the reaction between $CeCl_3$ and NaOH forming $Ce(OH)_3$, which transforms to CeO_2 in air. Second, the interaction between $ZrCl_4$ and NaOH yields high reactive amorphous ZrO_2. Then, the combining of *in situ* formed CeO_2 and amorphous ZrO_2 enables successful synthesis of ultrafine $Ce_{0.8}Zr_{0.2}O_2$. The reaction between the chemical precursors occurs during milling as a gradual transformation to the final product, which is embedded in the NaCl matrix. After 5 h of milling under energetic conditions, thermal treatment at low temperature (600 °C, 5 h) and further elimination of NaCl by washing conduces to the formation of nanostructured $Ce_{0.8}Zr_{0.2}O_2$ solid solution, with high surface area (26 $m^2\ gr^{-1}$). As an interesting result, when NaCl removal is performed before thermal treatment, the microstructural/textural characteristics of the $Ce_{0.8}Zr_{0.2}O_2$ solid solution were improved. A final material with a mesoporous network and a high surface area of 50 $m^2\ gr^{-1}$ is produced. This nanosized $Ce_{0.8}Zr_{0.2}O_2$ solid solution produced by a simple and versatile route is a promising active phase/support for different catalytic applications.

Acknowledgments

This study has been partially supported by CONICET (National Council of Scientific and Technological Research), CNEA (National Commission of Atomic Energy), ANPCyT (PICT N° 1049) and Instituto Balseiro (University of Cuyo). The authors thank to Carlos Cotaro for his assistance in the SEM observations.

References

[1] A. Trovarelli, Catalysis by Ceria and Related Materials, first ed., Imperial College Press, London, 1999.
[2] T. Omata, Y. Goto, S. Otsuka-Yao-Matsuo, Sci. Technol. Adv. Mater. 8 (2007) 524.
[3] J. Kaspar, P. Fornasiero, M. Graziani, Catal. Today 50 (1999) 285–298.
[4] J. Kaspar, P. Fornasiero, G. Balducci, R. Di Monte, N. Hickey, V. Sergo, Inorg. Chim. Acta 349 (2003) 217–226.
[5] P. Fornasiero, R. DiMonte, G.R. Rao, J. Kaspar, S. Meriani, A. Trovarelli, M. Graziani, J. Catal. 151 (1995) 168–177.
[6] G. Balducci, J. Kaspar, P. Fornasiero, M. Graziani, M.S. Islam, J.D. Gale, J. Phys. Chem. B 101 (1997) 1750–1753.
[7] H.-S. Roh, Y. Wang, D.L. King, A. Platon, Y.-H. Chin, Catal. Lett. 108 (2006) 15.
[8] J.L. Cao, Y. Wang, T.Y. Zhang, S.H. Wu, Z.Y. Yuan, Appl. Catal. B 78 (2008) 120.
[9] I. Dobrosz-Gómez, I. Kocemba, J.M. Rynkowski, Catal. Lett. 128 (2009) 297.
[10] K. Eguchi, N. Akasaka, H. Mitsuyasu, Y. Nonaka, Solid State Ionics 135 (2000) 589.
[11] Y.L. Chen, M. Qi, D.Z. Yang, K.H. Wu, Mater. Sci. Eng. A 183 (1994) L9.
[12] A. Trovarelli, F. Zamar, J. Llorca, C. de Leitenburg, G. Dolcetti, J.T. Kiss, J. Catal. 169 (1997) 490–502.
[13] A. Suda, T. Kandori, N. Terao, Y. Ukyo, H. Sobukawa, M. Sugiura, J. Mater. Sci. Lett. 17 (1998) 89.
[14] F.C. Gennari, T. Montini, P. Fornasiero, J.J. Andrade Gamboa, J. Hydrogen Energy 33 (2008) 3549–3554.
[15] H.S. Potdar, S.B. Deshpande, A.S. Deshpande, S.P. Gokhale, S.K. Date, Y.B. Khollam, A.J. Patil, Mater. Chem. Phys. 74 (2002) 306.
[16] H.T. Zhang, G. Wu, X.H. Chen, Mater. Chem. Phys. 101 (2007) 415.
[17] F.C. Gennari, A. Carbajal Ramos, A. Condó, T. Montini, S. Bengió, A. Cortesi, J.J. Andrade Gamboa, P. Fornasiero, Appl. Catal. A 398 (2011) 123–133.
[18] P. Nayak, B.B. Nayak, A. Mondal, Mater. Chem. Phys. 127 (2011) 12–15.
[19] C. Suryanarayana, Mechanical Allying and Milling, Marcel Dekker, New York, 2004.
[20] V.V. Zyryanov, Russ. Chem. Rev. 77 (2008) 105.
[21] T. Tsuzuki, P.G. McCormick, J. Mater. Sci. 39 (2004) 5143.
[22] A.C. Dodd, Mechanochemical Synthesis of Ceramics, in Chemical Processing of Ceramics, Second ed., CRC Press, 2005.
[23] D. Domanski, G. Urretavizcaya, F. Castro, F.C. Gennari, J. Am. Ceram. Soc. 87 (2004) 2020.
[24] T. Tsuzuki, P.G. McCormick, J. Am. Ceram. Soc. 84 (2001) 1453.
[25] S. Gopalan, S.C. Singhal, Scr. Mater. 42 (2000) 993.
[26] Y.X. Li, X.Z. Zhou, Y. Wang, X.Z. You, Mater. Lett. 58 (2003) 245.
[27] Y.X. Li, W.F. Chen, X.Z. Zhou, Z.Y. Gu, C.M. Chen, Mater. Lett. 59 (2005) 48.
[28] A.C. Dodd, T. Tsuzuki, P.G. McCormick, Mater. Sci. Eng. A 301 (2001) 54.
[29] A.C. Dodd, P.G. McCormick, Scr. Mater. 44 (2001) 1725.
[30] A.C. Dodd, P.G. McCormick, Acta Mater. 49 (2001) 4215.
[31] C. Cheng, Y.X. Li, X. Zhou, W. Chen, J. Rare Earths 22 (2004) 775.
[32] L.V. Moroova, A.E. Lapshin, T.I. Panova, V.B. Glushkova, Inorg. Mater. 38 (2002) 153 (translated from Neorganicheskie Materialy).
[33] J. Laugier, B. Bochu, LMGP-Suite Suite of Programs for the Interpretation of X-ray Experiments, ENSP/Laboratoire des Matériaux et du Génie Physique, BP 46. 38042 Saint Martin d'Hères, France, http://www.ccp14.ac.uk/tutorial/lmgp/.
[34] J.I. Langford, R.D.E. Delhez, T.H. H Keijser, E.J. Mittemeijer, Aust. J. Phys. 41 (1988) 173.
[35] M. Yashima, N. Ishizawa, M. Yoshimura, J. Am. Ceram. Soc. 7 (1992) 1550.
[36] K.S.W. Sing, D.H. Everett, R.A.W. Haul, L. Moscou, R.A. Pierotti, J. Rouquérol, T. Siemieniewska, Pure Appl. Chem. 57 (1985) 603.
[37] H.S.C. Outokumpu, Chemistry For Windows, Version 6.1. Outokumpu Research Oy, Finland, 2009.
[38] J. Livage, K. Doi, C. Mazières, J. Am. Ceram Soc. 51 (1968) 349.
[39] S. Gutzov, J. Ponahlo, C.L. Lengauer, A. Beran, J. Am. Ceram Soc. 77 (1994) 1649.
[40] T. Merle-Mkjeaqa, P. Barberiqb, S. Ben Othmane, F. Nardoua, P.E. Quintarda, J. Eur. Ceram. Soc. 18 (1998) 1579.
[41] M. Yashima, H. Arashi, M. Kakihana, M. Yoshimura, J. Am. Ceram. Soc. 77 (1994) 1067.